THE JOURNAL OF PHYSICAL CHEMISTRY B

Article

pubs.acs.org/JPCB

N-Acyl Chain in Ceramide and Sphingomyelin Determines Their Mixing Behavior, Phase State, and Surface Topography in Langmuir Films

Fernando G. Dupuy*,† and Bruno Maggio

Centro de Investigaciones en Química Biológica de Córdoba CIQUIBIC−CONICET/UNC, Departamento de Química Biológica, Facultad de Ciencias Químicas, Universidad Nacional de Córdoba. Haya de la Torre y Medina Allende, Ciudad Universitaria, X5000HUA Córdoba, Argentina

Supporting Information

ABSTRACT: Sphingolipids are membrane lipids composed by a long chain aminediol base, usually sphingosine, with a N-linked fatty acyl chain whose quality depends on the membrane type. The effect of length and unsaturation of the N-acyl chain on the mixing behavior of different sphingolipids has scarcely been studied, and in this work this issue is addressed employing Langmuir monolayers at the air−water interface, in order to assess the surface mixing in binary mixtures of different species of sphingomyelins and ceramides. The dependence on the monolayer composition of the mean molecular area, perpendicular dipole moment, domain segregation, and surface topography, as well as the film elasticity and optical thickness were studied. The results indicate that composition-dependent favorable interactions among sphingomyelin and ceramide occur as a consequence of complementary lateral packing and increased acyl chain ordering; the phase state of the components appears as a major factor determining miscibility among sphingomyelins and ceramides even in cases where the lipids have a considerable hydrocarbon chain length mismatch.

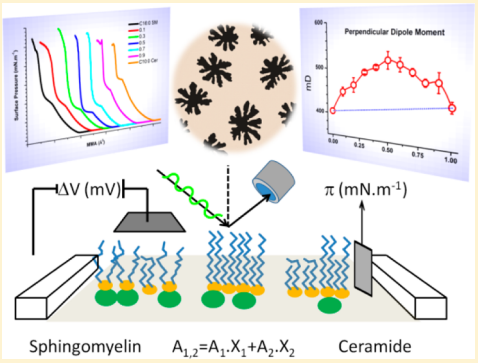

INTRODUCTION

Biological membranes are constituted by a complex mixture of lipids whose biochemical structure and metabolism regulate various aspects of membrane function such as fluidity, selective permeability, lateral diffusion, phase domain microheterogeneity, membrane protein folding, and sorting or even bilayer destabilization during membrane fusion and fission events.

Among the different membrane components, sphingolipids comprise a large family characterized by a long-chain aminediol base, with a fatty acyl moiety N-bonded by amide linkage. Polar residues such as phosphocholine and various types of carbohydrates can be attached to the hydroxyl group at position 1 of the sphingoid base.[1−3] Thus, hydrogen bond donor and acceptor groups can be located at the interfacial plane and in the polar headgroup region of sphingolipids.[4] The most usually found base is sphingosine with a length of 18 carbons and one trans-unsaturation at position 4−5, whereas a larger variety in length, hydroxylation, and unsaturation can be found in the N-linked fatty acyl chain.[1−3,5,6]Bilayer interdigitation may be brought about by hydrocarbon chain length asymmetry between the sphingosine base and the N-bonded fatty acyl residue.[7−9]

The simplest kind of two-chained sphingolipids, ceramides, contain a single hydroxyl group in position 1 of the sphingoid and the most abundant species, although present in relatively low amounts in biological membranes are those containing N-acylated saturated fatty acyl chains of 16 or 18 carbons in length.[10] Being some of the lipids with the highest transition temperatures (~90 °C),[11,12] they are implicated in the formation of various types of highly ordered lipid domains in rather solid states,[13−15] although fluid states, phase transitions, and phase coexistence were also reported.[16] Those properties are a consequence of favorable close packing of the molecules, allowing enhanced van der Waals interactions between the hydrocarbon chains and stabilizing hydrogen bonding networks at the interface.[4,17] High amounts of ceramides N-acylated with long, hydroxylated fatty acid are encountered stacked in multilayers mixed with cholesterol and free fatty acids at the stratum corneum of the skin, preventing water passage and maintaining structural integrity.[18−20]

Sphingomyelins, on the other hand, contain a phosphocholine group at the OH of position 1 of ceramide. This phosphosphingolipid is a major constituent of the plasma membrane of eukaryotic cells,[21] and it has also been involved in the formation of ordered domains upon interaction with ceramide and cholesterol.[22] However, the phosphocholine polar group impairs a tight packing of sphingomyelin molecules when compared to ceramides N-acylated with the same fatty acid, thus leading to lower transition temperatures.[1,10,12,21,23] On the other hand, natural sphingomyelin extracts exhibit

Received: February 17, 2014
Revised: June 19, 2014
Published: June 20, 2014

phase transitions between ordered/disordered states at physiological temperatures, owing also to the occurrence of N-linked long/saturated fatty acyl chains.[6,21]

In sphingolipid metabolism, ceramide is a pivotal compound of high significance for metabolic signaling.[24,25] It represents a converging point for both the synthetic and degradative pathways of glycosphingolipids[5,26] and also regulates the content of diacylglycerol,[27−29] of some glycerophospholipids, and of other lipid messengers, such as the platelet activating factor. In such metabolic neworks, a sequence of transacetylase reaction activities are involved in the interconversion of C2-Cer with ceramides with different chain lengths in cells and tissues.[3,30] On the other hand, molecular species of natural ceramides are metabolically connected to sphingomyelins through the activity of different sphingomyelinases that remove the phosphocholine group irrespective of the N-acyl chain length of the substrate.[31,32] Also, some of these enzymes are endowed of phospholipase-A2-like activities that lead to the modification of glycerophospholipids hydrocarbon chain composition. Thus, difficulties in the evaluation of the effect of a particular lipid in a cellular scenario can arise not only from the complex composition of the membranes but also from the relationships among several metabolic networks.[33]

A rather widespread idea of the functional importance of sphingolipids in cell membranes refers to the occurrence of ordered domains enriched in sphingomyelin and ceramide, that are assumed to exist irrespectively of the possible influence of the of type of N-acyl chain in these lipids. However, most studies dealing with such condensed and ordered domains employ compounds with acyl chains with 16 carbons, while less attention has been devoted to understand the influence of variations of the N-acyl chain on the phase state and miscibility of lipids, either in model or natural membranes. Actually, it is frequently disregarded that *N*-palmitoyl-ceramide itself exhibits rich temperature- and surface pressure-dependent phase transitions among various condensed and expanded states of different organization and thickness.[16,34] Besides, relatively small variations of the N-acyl chain length of ceramides markedly affects their phase state, interfacial elasticity and thickness, surface topography, and electrostatics;[35] and even condensed ceramides can form liquidlike expanded states when interacting with ceramides with particular hydrocarbon chain mismatch.[36]

The interaction of some species of sphingomyelin and ceramide has been studied before in monolayers[37] and bilayers.[37,38] Ceramide forms condensed domains segregated from fluid phases enriched in sphingomyelin[37] and unsaturated phosphatidylcholines,[39,40] even in the presence of low amounts of cholesterol,[41] leading to the idea that ceramide and cholesterol can compete in ordered domains with sphingomyelin.[42,43] Mixtures of ceramides and sphingomyelins N-acylated with palmitic acid (C16:0) at the air−water interface showed a thermodynamically stable point at $X_{C16:0\ Cer} = 0.4$ with molecular area condensation, whereas in bilayer systems, complex DSC thermograms were reported,[37] with increasing melting temperatures at an increasing ceramide content. A similar behavior was also reported for mixtures of C16:0 sphingomyelin with C12:0, C18:0, and even C24:1 ceramides.[38] On the other hand, the interaction with the shorter N-acyl chain length C4:0 and C8:0 ceramides resulted in complex thermograms but at decreasing temperatures. By means of nuclear magnetic resonance, Leung et al. measured the specific melting of C16:0 sphingomyelin and C16:0 ceramide upon gel-to-liquid crystalline phase transition by using perdeuterated palmitic acid N-acylated in either ceramide or sphingomyelin;[44] it was demonstrated that ceramide-induced gel-phase stabilization by hydrocarbon chain ordering upon mixing and melting of the sphingomyelin component at slightly lower temperatures.

The aim of this work is to further understand how the heterogeneity of the N-acyl chain can regulate the miscibility of sphingomyelin and ceramide and their propensity to form mixed interfaces with segregated coexisting domains in different phase states. The interaction of ceramides and sphingomyelins with defined N-acyl chain lengths under well-controlled conditions of lateral organization was studied for this purpose. The dependence of molecular packing, in-plane elasticity, pressure-induced phase transition, surface (dipole) potential, and surface topography with the composition of binary mixtures were directly determined employing compression isotherms and Brewster angle microscopy on Langmuir monolayers. The results obtained indicate that, contrary to a common general assumption, the presence of ceramide does not always lead to formation of rather solid segregated domains. The surface behavior and miscibility of sphingomyelin and ceramide are selectively dependent on the type of the amide-linked hydrocarbon chain present in both lipids as well as on their relative phase state and proportions in the mixture.

MATERIALS AND METHODS

The sphingolipids *N*-decanoyl-D-*erythro*-sphingosine (C10:0 ceramide), *N*-palmitoyl-D-*erythro*-sphingosine (C16:0 ceramide), *N*-lygnoceroyl-D-*erythro*-sphingosine (C24:0 ceramide), *N*-nervonoyl-D-*erythro*-sphingonsine (C24:1 ceramide), *N*-lauroyl-D-*erythro*-sphingosylphosphorylcholine (C12:0 sphingomyelin), *N*-palmitoyl-D-*erythro*-sphingosylphosphorylcholine (C16:0 sphingomyelin) and *N*-lignoceroyl-D-*erythro*-sphingosylphosphorylcholine (C24:0 sphingomyelin) were purchased from Avanti Polar Lipids and used without further purification. Lipid stock solutions were prepared in chloroform:methanol (9:1) and stored at −72 °C until use. Working day solutions and mixtures were prepared in Teflon coated-cap tubes (Corning) and kept at −20 °C to minimize solvent evaporation. Handling of lipid solutions was carried out with Hamilton syringes. Solvents were HPLC-grade (Merck) and water was treated by successive passage through two water purification devices (Elix 10 and Gradient A10, Millipore), thus yielding a product with resistivity of 18.2 MΩ cm.

Langmuir monolayer experiments were carried out in a KSV Minitrough system (KSVNIMA, Biolin Scientific) equipped with a 270 cm^2 Teflon trough, Delrin barriers, surface potential device (SPOT, KSVNIMA), and temperature control by means of an external circulating water bath (Haake F3C). The whole system was kept enclosed in an acrylic box covered with a Faraday protection cage in order to avoid dust contamination and reduce external interference on the surface potential measurements.

The monolayers of lipids at air−water interface were prepared by dropwise deposition of the lipid solutions with a Hamilton syringe onto the surface of a 145 mM NaCl solution in a Teflon trough. Absence of surface-active impurities in the subphase solution or in the spreading solvents was ascertained, as described elsewhere.[35] Compression isotherms at a constant rate of compression of 5 $Å^2$ $molec^{-1}$ min^{-1} were started after 5 min of film spreading in order to allow for solvent evaporation.

dx.doi.org/10.1021/jp501686q | J. Phys. Chem. B 2014, 118, 7475−7487

Brewster angle microscopy of the monolayers was performed with an autonulling imaging ellipsometer (Nanofilm EP3sw, Accurion) equipped with 10× and 20× objectives and set up on a KSV Minitrough. Probe-free imaging of the monolayers was achieved by measuring the reflectivity of a *p*-polarized laser radiation (532 nm) incident at Brewster angle onto the film surface. In the presence of phases with different optical characteristics, the reflectivity of the different regions of the surface were determined separately by measuring the gray level of each phase with ImageJ (1.43μ Wayne Rasband−NIH).

Monolayer phase transitions were calculated from the changes of the slope of the surface pressure (π)-mean molecular area (A) isotherms with the method of second and third derivatives of the monolayer compression isotherms[45] in a personal computer with Origin software. The crude isotherms are shown in the figures. For further calculations, data were interpolated at constant molecular area increments of 0.1 Å and smoothed by means of Savitsky−Golay algorithms previous to mathematical processing.

The in-plane elasticity of the films at a particular surface pressure is reflected by the surface compressibility modulus (C_s^{-1}):[46]

$$C_S^{-1} = -A\frac{\delta\pi}{\delta A}$$

For mixed films, an ideal elasticity was calculated[47] considering that the components maintain their own compressibility and mean molecular area in the mixture.

$$C_S^{-1}|_\pi = (X_1A_1 + X_2A_2)\left(\left(X\frac{A}{C_s^{-1}}\right)_1 + \left(X\frac{A}{C_s^{-1}}\right)_2\right)_\pi^{-1}$$

where X_n, A_n and C_s^{-1} are the molar fraction, mean molecular area, and surface compressibility modulus of the n component at the surface pressure π, respectively.

Surface electrostatic measurements at different surface pressures were used to determine the resultant perpendicular dipole moment ($\mu_\perp$) of the monolayers[46,48] according to

$$[\mu_\perp]_\pi = \left[\frac{1}{37.7}A\Delta V\right]_\pi$$

where A is the mean molecular area at a particular surface pressure and ΔV is the difference of the surface (dipole) potential of the film at different surface pressures (π) compared to that of the clean subphase.

The resultant perpendicular dipole moment of the mixed films is compared with that of an ideal mixture calculated at each surface pressure with an additivity equation:[46]

$$[\mu_{\perp_m}]_\pi = [X_1(\mu_1) + X_2(\mu_2)]_\pi$$

Lateral packing of the molecules at the air−water interface is directly determined from the surface area occupied by the film and the number of molecules spread. The mean molecular area of the mixtures at a particular surface pressure is compared to that corresponding to an ideal mixing of the components, which follows an additivity rule:[46]

$$[A_m]_\pi = [X_1A_1 + X_2A_2]_\pi$$

The free-energy of monolayer compression was calculated from the integral of π−A curves between 1 and 35 mN m^{-1}, and the excess function in mixtures was obtained as the difference between the free energy of compression for the mixture and that of the ideal mixture the components:[46]

$$\Delta G_{excess} = \int_1^{35}[A_m - (X_1A_1 + X_2A_2)]d\pi$$

RESULTS

C16:0 Ceramide/C16:0 Sphingomyelin. In previous studies, favorable interactions were described in the mixture of C16:0 sphingomyelin and C16:0 ceramide:[37] mean molecular area condensation (Figure S2B of the Supporting Information) and hyperpolarization (Figure S2D of the Supporting Information) compared to the ideal mixing behavior (Figure S2 of the Supporting Information, dotted lines) were observed. However, the π vs A isotherms of the mixtures with $X_{Cer} < 0.3$ showed a shoulder at 18 mN m^{-1} that corresponds to the expanded-condensed transition of pure C16:0 sphingomyelin (Figure S1A of the Supporting Information), indicating at least partial miscibility of pure sphingomyelin. Even at the lowest $X_{C16:0\ Cer}$ assayed and at surfaces pressures below 18 mN m^{-1} (Figure S3, panels G and H, of the Supporting Information), BAM images revealed the coexistence of a bright condensed phase enriched in ceramide with a darker expanded phase (Figure S3, panels D and E, of the Supporting Information). Also, both phases remain separated at higher surface pressures, in the condensed state of the film. However, at $X_{C16:0\ Cer}$ higher than 0.4, monolayer appeared mostly condensed either at low or high surface pressures (Figure S3F of the Supporting Information).

Binary Mixtures of C16:0 Sphingomyelin with C24:0 Ceramide and C10:0 Ceramide. In a previous work on the effect of the hydrocarbon chain mismatch in the mixing behavior of ceramides in Langmuir monolayers, it was found that a mismatch of 2 carbons in the N-acyl chain length led to total miscibility whereas a difference of 4 and 6 carbons caused partial and full immiscibility, respectively.[36] However, the interaction of C16:0 Sphingomyelin with ceramides N-acylated with saturated longer or shorter chain fatty acids produced mixed films with expanded phases (Figure 1). The compression isotherms of the mixtures with the saturated-long chain C24:0 Ceramide displayed a slightly defined transition pressure that rapidly decreased to lower surface pressures (Figure 1A) when the ceramide content in the films was increased up to $X_{C24:0\ Cer}$ = 0.1 (Figure 1A, arrows, see also Figure 3D). The unexpected miscibility of this highly condensed ceramide with the expanded phase of C16:0 Sphingomyelin was also confirmed by BAM: at surfaces pressures and compositions below the phase transition, the film appeared homogeneous, whereas domains of condensed phase started to grow when the surface pressure of the mixed films was increased above the transition surface pressure of the monolayers (Figure 2A, left panel). When the ceramide content in films was increased above 10%, presence of the condensed state was observed at all surface pressures (Figure 2A, right panel). Similar to the mixture C16:0 Ceramide/C16:0 Sphingomyelin, the monolayer expanded-condensed transition of the sphingomyelin can still be observed at $0 < X_{C24:0\ Cer} < 0.5$ (Figure 1A), indicating that a sphingomyelin-enriched mixture is phase separated from the rest of the mixed film. At higher $X_{C24:0\ Cer}$ condensed mixed films are formed with featureless compression isotherms.

On the other hand, the hydrocarbon chain length mismatch between sphingomyelin/ceramide obtained when the N-acyl chain of the ceramide is shortened from 16 to 10 carbons

dx.doi.org/10.1021/jp501686q | J. Phys. Chem. B 2014, 118, 7475−7487

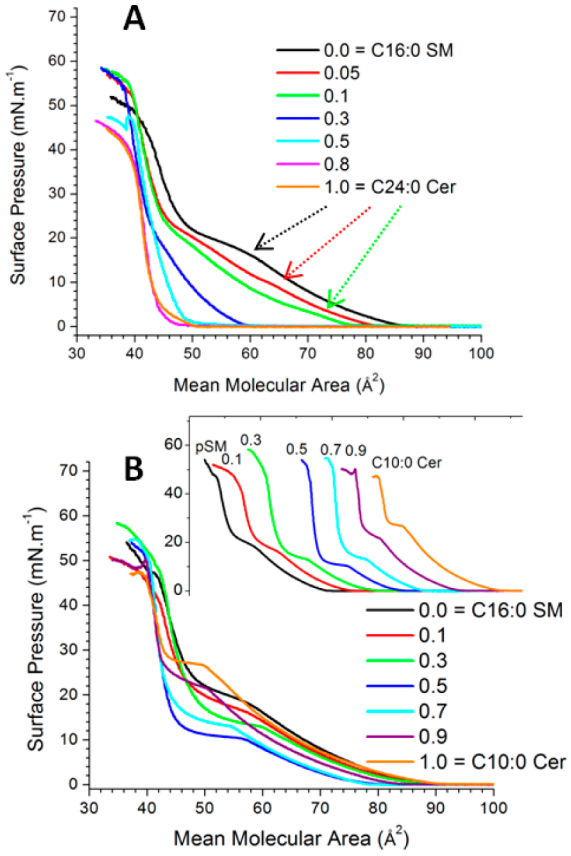

Figure 1. Compression isotherms of binary mixtures of C16:0 Sphingomyelin with C24:0 Ceramide (A) and C10:0 Ceramide (B). Arrows in A) indicate the monolayer transition of the mixed expanded phase formed with the long chain C24:0 Ceramide; the inset in B shows isotherms offset along the abscissa in order to point out the decrease of the transition surface pressure with the composition in the mixture of the C16:0 Sphingomyelin with the short chain C10:0 Ceramide.

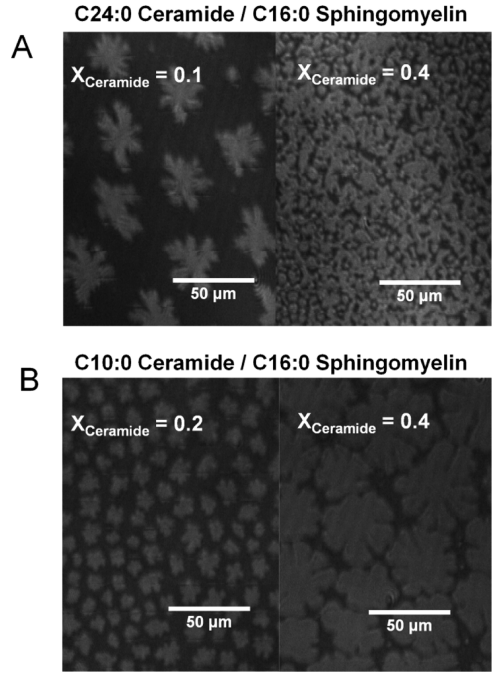

Figure 2. Monolayer imaging by BAM of the mixtures at 15 mN $m^{-1}$of C16:0 Sphingomyelin with C24:0 Ceramide (A) and C10:0 Ceramide (B).

resulted in a complete miscibility of C10:0 Ceramide with C16:0 Sphingomyelin in the expanded phase over the whole compositional range, as indicated by a single transition surface pressure in the π–A isotherms (Figure 1B). Also, the transition surface pressure of the mixtures changed with the film composition as expected for a good miscibility but reached a minimum of 10 mN m^{-1} at the equimolar ratio, which is under the transition pressure of both, namely 24 mN m^{-1} for C10:0 Ceramide and 18 mN m^{-1} for C16:0 Sphingomyelin (Figure 3D). This indicates that, in those proportions, the components interact more strongly in the mixture than in the pure state, facilitating (lower transition surface pressure) the formation of a condensed phase in the mixed film.

BAM measurements revealed the formation of flower-like domains of condensed phase in the phase transition region; these increased in size as the monolayer area was reduced (Figure 2B), suggesting a two-dimensional diffusion-limited mechanism for domain growth. Also, the domain size inversely correlated with the transition surface pressure of the film, showing the largest domains in the mixtures with 0.4 < $X_{C16:0\ Cer}$< 0.6 (Figure 2B, right panel) when compared to those formed in the mixtures enriched in either of the components.

The binary mixtures of C16:0 Sphingomyelin with the asymmetric lipids C10:0 Ceramide and C24:0 Ceramide showed mean molecular area condensation. At 5 mN m^{-1}, the C16:0 sphingomyelin/C10:0 Ceramide films were even more condensed than either of the components (Figure 3A) reaching a minimum lateral area of 64 Å^2, significantly lower than the value of 81 Å^2 predicted by the additivity rule, at the composition of 0.5< $X_{C10:0\ Cer}$< 0.7. In the case of the C24:0 Ceramide/C16:0 Sphingomyelin mixture, the mean area of films with 50% of C24:0 Ceramide was 46 Å^2, a value which is more similar to the area of the ceramide than to that of the sphingomyelin (42 and 74 Å^2, respectively, Figure 3A).

At surface pressures above 30 mN m^{-1}, at which both components are in the condensed state, the amount of condensation of the mean molecular area was not significant. The analysis of the elasticity of the films, however, also suggested interactions in the mixed films of C24:0 Ceramide/C16:0 Sphingomyelin and of C10:0 Ceramide/C16:0 Sphingomyelin: both mixed films showed higher surface compressibility modulus when compared to the predicted theoretical behavior (Figure 3B). The nonideal stiffening of the interface was higher in the case of the mixture of C16:0 Sphingomyelin with C10:0 Ceramide than for C24:0 Ceramide: the modulus of the equimolar mixture of C10:0 Ceramide/C16:0 Sphingomyelin more than doubled the theoretically predicted values (490 vs 190 mN m^{-1}, respectively, Figure 3B), whereas in the case of the C24:0 Ceramide/C16:0 Sphingomyelin mixture, the measured elasticity was only about 40% more than the ideal value (330 and 230 mN m^{-1}, respectively, Figure 3B).

The average perpendicular dipole moment of the mixtures at 30 mN m^{-1} also indicated molecular interactions between C16:0 Sphingomyelin and the asymmetric ceramides: hyperpolarization of the interface in both mixtures when compared to the ideal behavior was observed. The perpendicular dipole moment increased with the proportion of either C10:0 or C24:0 ceramide and reached comparable values to those of pure ceramide at $X_{Ceamider}$= 0.6 (Figure 3C).

dx.doi.org/10.1021/jp501686q | J. Phys. Chem. B 2014, 118, 7475−7487

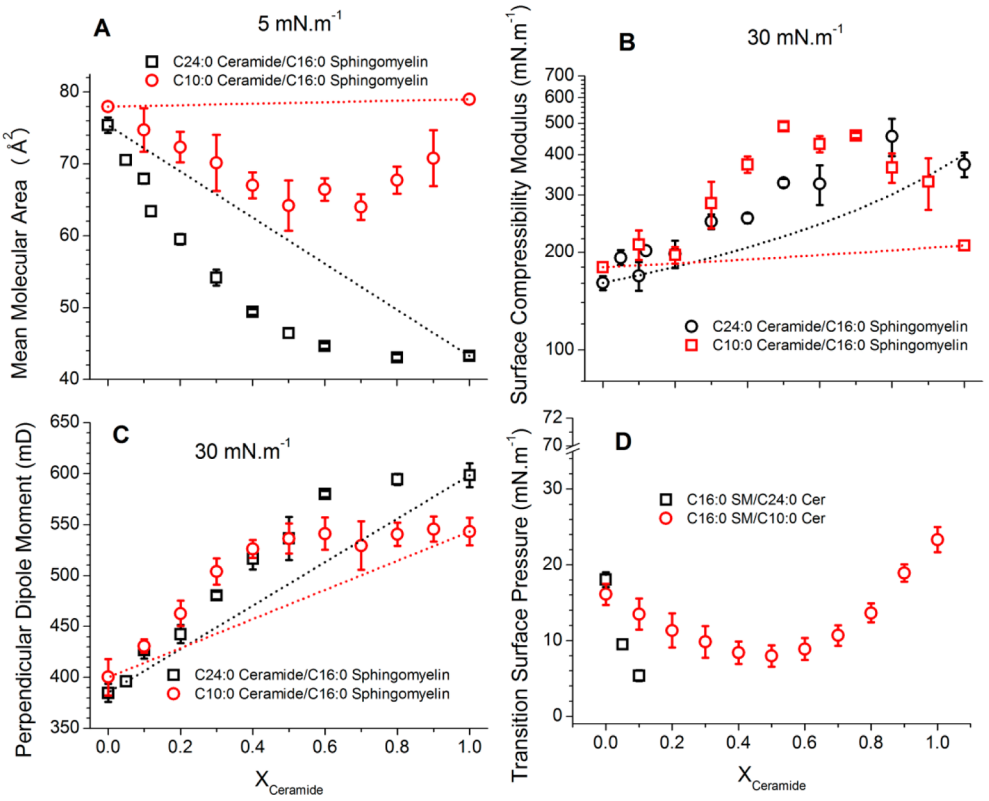

Figure 3. Variation with the film composition of the mixing parameters Mean Molecular Area (A), Surface Compressional Modulus (B), Perpendicular Dipole Moment (C) and Transition Surface Pressure (D) of the binary mixtures of C16:0 Sphingomyelin with C24:0 and C10:0 Ceramide.

Highly Mismatched Mixtures: C24:0 Ceramide/C12:0 Sphingomyelin and C10:0 Ceramide/C24:0 Sphingomyelin. In order to get further insights on the effect of the N-acyl chain in sphingomyelin/ceramide interactions, two mixtures with a high mismatch in the N-acyl chain length were studied: mixed films of the fully expanded C12:0 Sphingomyelin with the fully condensed C24:0 Ceramide, and mixtures of C24:0 Sphingomyelin (showing a phase transition at 4 mN m^{-1}) with C10:0 Ceramide (also showing a phase transition but at 24 mN m^{-1}) were analyzed.

The compression isotherms of the C24:0 Ceramide/C12:0 Sphingomyelin mixtures were featureless and exhibited no phase transition (Figure 4A) with only a smooth decrease of the molecular area at increasing ceramide contents in the films.

On the other hand, the mixture of C10:0 Ceramide/C24:0 sphingomyelin formed monolayers with only one, highly cooperative, transition from expanded to condensed states reflected by the rather horizontal plateau of the isotherms over the phase coexistence region (Figure 4B); this indicates a good miscibility both in the expanded and in the condensed states even despite the hydrocarbon chain mismatch of the components. The transition surface pressure displayed a complex behavior with the film composition: from $X_{C10:0\ Cer}$ = 0.0 to 0.5 it increased with a small slope from 4 to 6 mN m^{-1}, while at $X_{C10:0\ Cer}$ > 0.5 it increased steeply from 6 up to 24 mN m^{-1} at $X_{C10:0\ Cer}$= 1.0 (Figure 5D).

The mixing parameters showed only small deviations from the ideal behavior for the C24:0 ceramide/C12:0 sphingomyelin mixture: the mean molecular area at 5 mN m^{-1}(Figure 5A) and perpendicular dipole moment (Figure 5C) at 30 mN m^{-1}, essentially followed the additivity rule. On the other hand, the mean molecular area of the C10:0 ceramide/C24:0 sphingomyelin mixture showed slight but siginificant deviations from the predicted behavior: positive deviation in the expanded state at 3 mN m^{-1} at $X_{C10:0\ Cer}$ < 0.4 but condensation at higher ceramide contents (Figure 5A). The surface compressibility modulus showed slight positive deviations at 30 mN m^{-1} and at X_{Cer} > 0.3 when compared to the predicted values for the C24:0 ceramide/C12:0 sphingomyelin mixture (Figure 5B), whereas for the C10:0 ceramide/C24:0 sphingomyelin mixture, it indicated considerable film stiffening when compared to the predicted values (Figure 5B). Accordingly, the surface electrostatics of the films of C10:0 ceramide/C24:0 sphingomyelin at 30 mN m^{-1} also revealed hyperpolarization of the mixed monolayers compared to the ideal mixture (Figure 5C).

BAM imaging of the mixed films confirmed the different behavior of the two mismatched mixtures: while the C24:0 ceramide/C12:0 sphingomyelin system exhibited expanded-condensed phase coexistence over the whole range of composition, both at low and at high surface pressures (Figure 6, left panel), the C10:0 ceramide/C24:0 sphingomyelin mixture showed a homogeneous expanded phase at surface pressures under the transition pressure (Figure 6, middle panel). Round-shaped domains of condensed phase appeared at surface pressures above the phase transition of the mixed films of C10:0 ceramide/C24:0 sphingomyelin and increased in size upon further compression (Figure 6, right panel). The domains also showed decreasing reflectivity levels at increasing contents of ceramide.

Binary Mixtures of C24:1 Cer with C12:0 SM, C16:0 SM, and C24:0 SM. The results obtained suggest that sphingomyelin and ceramide interact favorably in binary

dx.doi.org/10.1021/jp501686q | J. Phys. Chem. B 2014, 118, 7475−7487

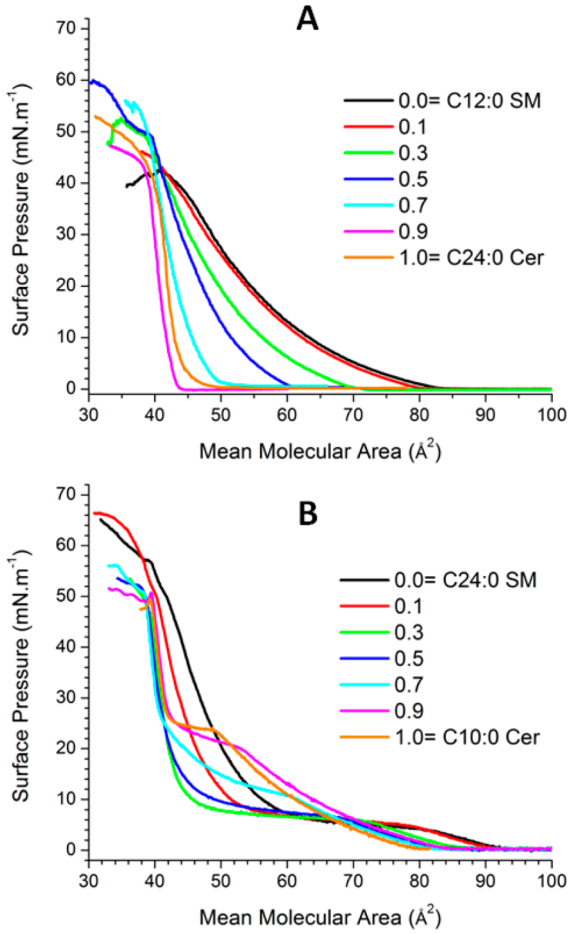

Figure 4. Compression isotherms of binary mixtures of sphingomyelins and ceramide with a high mismatch in the N-acyl chain length. (A) C12:0 sphingomyelin/C24:0 ceramide appears rather immiscible, whereas (B) C24:0 sphingomyelin/C10:0 ceramide formed mixed expanded phases over the whole range of compositions.

mixtures even in the presence of high hydrophobic mismatch of the N-acyl chain length. However, only the asymmetric short-chain C10:0 ceramide-induced condensation and stiffening of the films when mixed both with C16:0 or with C24:0 sphingomyelin. In order to assess if the long chain C24:0 ceramide did not mix with C12:0 sphingomyelin as a consequence of the mismatch in the N-acyl chain length or in the different film elasticity, the mixing behavior of the nervonic N-acylated ceramide (C24:1 ceramide) was studied. The latter is a long chain lipid but with an unsaturation that introduces disorder in the hydrocarbon chains.

At variance with C24:0 ceramide, the interaction of C12:0 sphingomyelin with the long N-acyl chain C24:1 ceramide produced well mixed expanded monolayers (Figure 7A) with expanded/condensed transition at decreasing surface pressures in proportion to the content of C24:1 Cer (from 24 mN m^{-1} at $X_{C24:1\ Cer}$ = 0.2 to less than 1 mN m^{-1} at $X_{C24:1\ Cer}$ = 0.7, Figure 8D), indicating that the diminished solid character of the C24:1 ceramide facilitates its interaction and mixing with the short chain sphingomyelin.

However, increasing the N-acyl chain length of the sphingomyelin, thus reducing the hydrophobic mismatch between the molecules, enhanced the molecular interactions in the mixtures with C24:1 ceramide: mixed expanded phases with well-defined, cooperative expanded to condensed monolayer phase transition, indicating good miscibility in the expanded state, were observed in films of C24:1 ceramide/C16:0 sphingomyelin (Figure 7B); whereas, a full condensation of the C24:0 sphingomyelin isotherms occurred at $X_{C24:1\ Cer}$ = 0.4 (Figure 7C).

The degree of mean molecular area condensation at 3 mN m^{-1} (Figure 8A), film stiffening (Figure 8B), and hyperpolarization (Figure 8C) of the interface induced at 30 mN m^{-1} by C24:1 ceramide in the different mixtures is higher the smaller the hydrophobic mismatch, in the order C24:0 sphingomyelin > C16:0 sphingomyelin > C12:0 sphingomyelin. Compared to the ideal behavior, the mean molecular areas of the mixture with C12:0 sphingomyelin were more expanded at $X_{C24:1\ Cer}$ < 0.6 and showed significant condensation only at $X_{C24:1\ Cer}$ > 0.8 (Figure 8A). On the other hand, the mixtures with C16:0 and C24:0 sphingomyelin were more condensed compared to the theoretical behavior over the whole compositional range and reached maximum condensation at $X_{C24:1\ Cer}$ = 0.6 and 0.3, respectively (Figure 8A).

The increase of the surface compressibility modulus at 30 mN m^{-1} followed a similar trend than the decrease in area: the C24:1 ceramide/C12:0 sphingomyelin films were stiffer than the ideal mixture at $X_{C24:1\ Cer}$ > 0.3 (Figure 8B), whereas the mixtures of C24:1 ceramide with C16:0 and C24:0 sphingomyelin showed a surface compressibility module significantly higher than the predicted values over the whole compositional range and more pronounced in the mixture of C24:1 ceramide/C24:0 sphingomyelin (Figure 8B), representing the highest values among all the mixtures studied.

The analysis of the surface electrostatics revealed also a strong hyperpolarization of the mixed films of C24:1 ceramide with the different sphingomyelins, being the magnitude of the effect in correspondence with the increase of the surface compressibility modulus, indicating a closer molecular packing and higher degree of interactions in mixtures with smaller hydrophobic mismatch (Figure 8C).

BAM measurements confirmed the mixed expanded phase formed in the mixtures of C24:1 ceramide and C12:0 and C16:0 sphingomyelin. At surface pressures under that of the monolayer transition, the films appeared dark and homogeneous with no sign of a bright, condensed phase of the ceramide, indicating the absence of pure C24:1 Cer in the condensed state. At surface pressures above that of the phase transition, flower-shaped domains with reflectivity levels higher than those of the pure components were observed (Figure 9). Upon film compression, the domains increased in size and also in mixtures increasingly enriched in ceramide, thus inversely correlated with the transition surface pressure. Also, the largest domains observed among all the mixtures studied corresponded to those observed in the mixture C24:1 ceramide/C16:0 sphingomyelin (BAM pictures were taken at 10× objective in the latter case, at variance with the other mixtures, in which a 20× magnification was used; compare scale bar in the left and middle panel of Figure 9).

In the case of the C24:1 ceramide/C24:0 sphingomyelin mixture, the film surface appeared bright and homogeneous at the micrometric resolution of BAM over the whole range of composition and surface pressures (Figure 9, right panel). The reflectivity levels of the mixed films were higher than those of single component films, following a similar dependence with the composition to the perpendicular dipole moment.

dx.doi.org/10.1021/jp501686q | J. Phys. Chem. B 2014, 118, 7475−7487

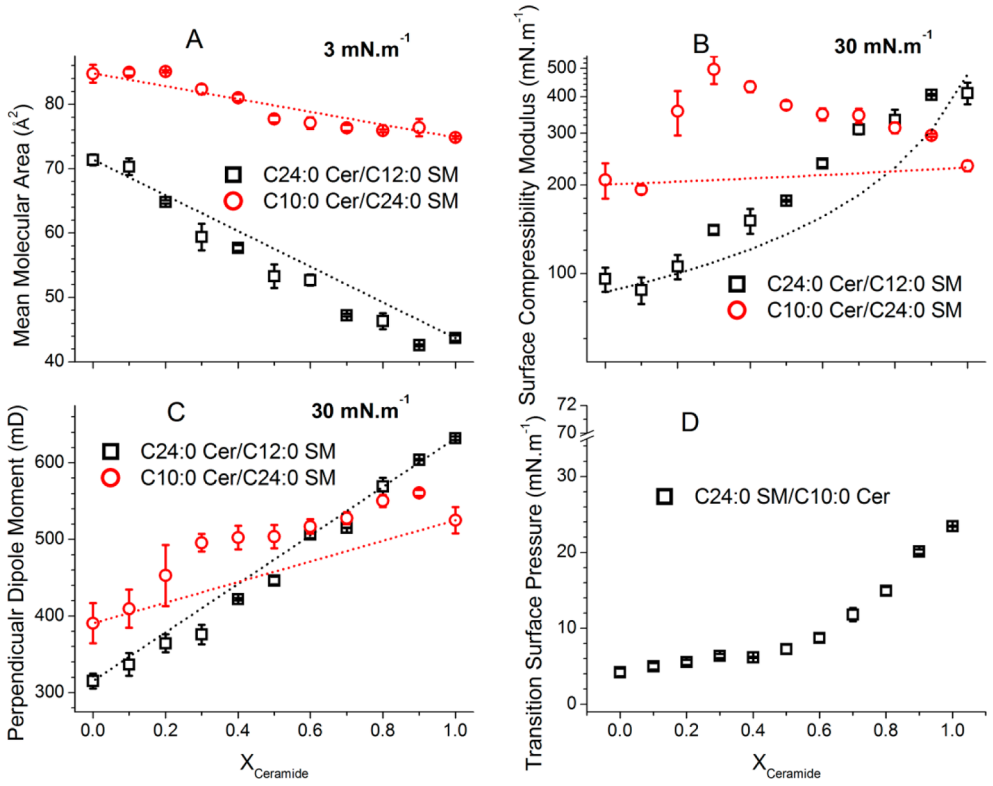

Figure 5. Variation on the film composition of the mixing paramenters (A) mean molecular area, (B) surface compressional modulus, (C) perpendicular dipole moment, and (D) transition surface pressure of the binary mixtures C12:0 sphingomyelin/C24:0 ceramide and C24:0 sphingomyelin/C10:0 ceramide.

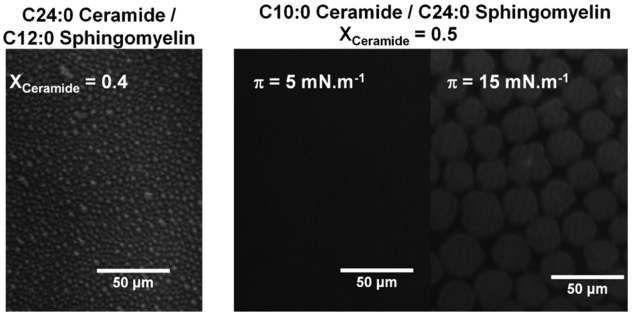

Figure 6. Monolayer imaging by BAM of the mixtures C12:0 sphingomyelin/C24:0 ceramide at 15 mN m^{-1} and C24:0 sphingomyelin/C10:0 ceramide at 5 and 15 mN m^{-1}.

DISCUSSION

As indicated in previous studies,[35,36,49] the length and unsaturations of the N-acyl chain is a major determinant of the surface behavior of ceramides and sphingomyelins. Ceramides form more condensed films in Langmuir monolayers than sphingomyelins N-acylated with the same fatty acid, showing both lower transition surface pressures and higher compressibility modulus: C12:0 sphingomyelin is fully expanded (Figure S1 of the Supporting Information), whereas C12:0 ceramide undergoes a phase transition at 3.9 mN m^{-1};[35] C16:0 sphingomyelin shows a phase transition at 18 mN m^{-1} (Figure S1 of the Supporting Information) and C16:0 ceramide is fully condensed,[35] with surface compressibility modulus of 260 mN m^{-1} and 380 mN m^{-1} at a surface pressure of 35 mN m^{-1}, respectively. Also, similar expanded to condensed

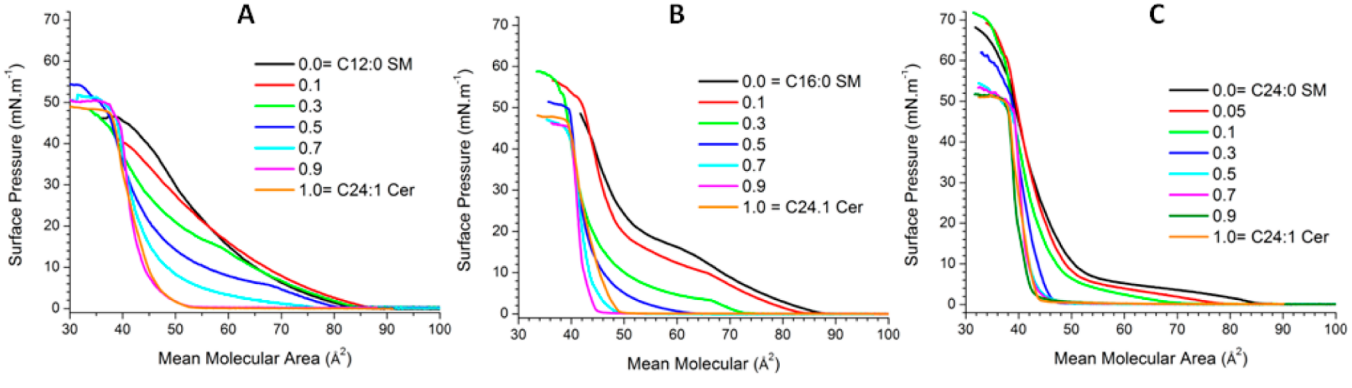

Figure 7. Compression isotherms of binary mixtures of C24:1 ceramide with (A) C12:0, (B) C16:0, and (C) C24:0 sphingomyelin.

dx.doi.org/10.1021/jp501686q | J. Phys. Chem. B 2014, 118, 7475−7487

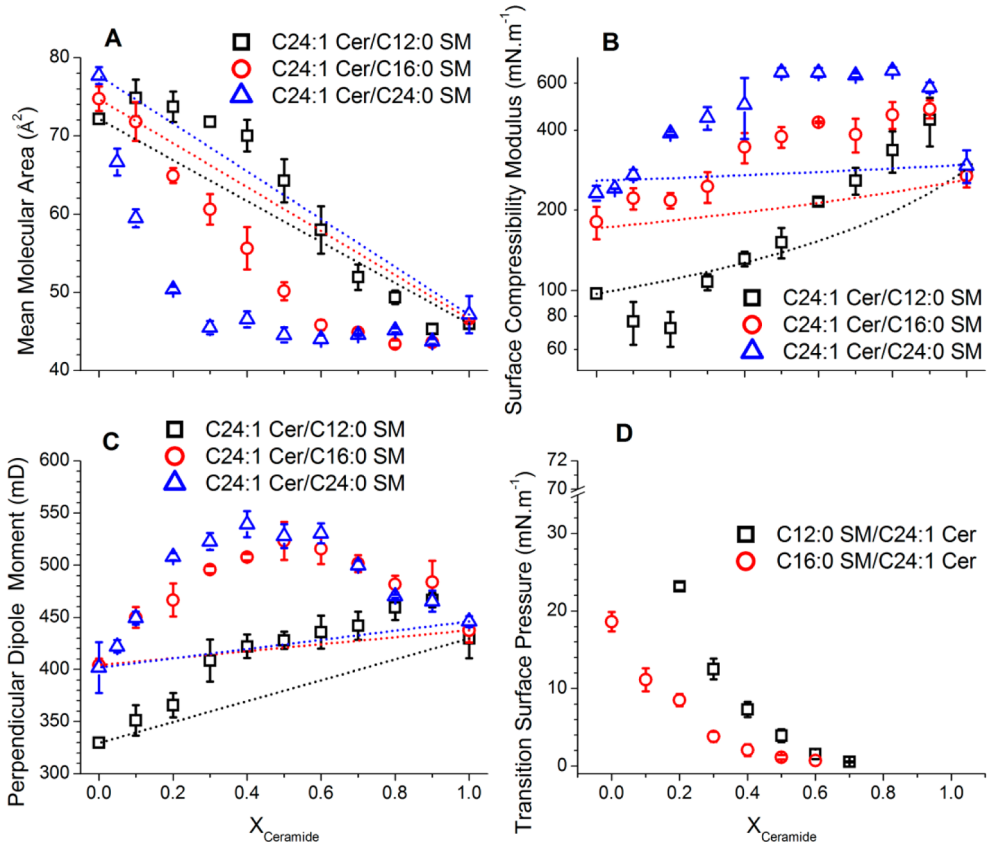

Figure 8. Variation with the film composition of the mixing paramenters (A) mean molecular area, (B) surface compressional modulus, (C) perpendicular dipole moment, and (D) transition surface pressure of the binary mixtures of C24:1 ceramide with C12:0, C16:0, and C24:0 sphingomyelin.

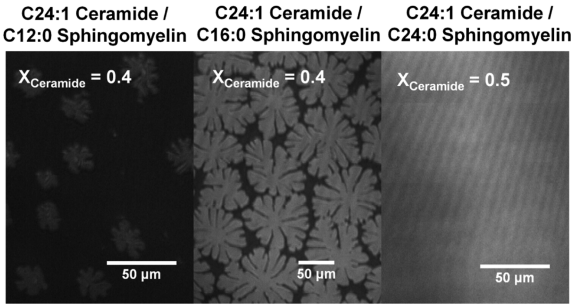

Figure 9. Monolayer imaging by BAM of the mixtures of C24:1 ceramide with C12:0, C16:0, and C24:0 sphingomyelin at 15 mN m^{-1}.

transition surface pressures in monolayers are encountered in sphingomyelins with 4 to 6 carbons longer N-acyl chains than ceramides with the same sphingosine chain: C14:0 sphingomyelin and C10:0 ceramide show an expanded-condensed transition at 30 and 24 mN m^{-1}, respectively, whereas for C18:0 sphingomyelin and C12:0 ceramide, it is found at about 3 mN m^{-1}.[35,49] This reflects that in sphingomyelin, the presence of the bulkier, more hydrated phosphocholine group prevents a closer packing of hydrocarbon chains, and the absence of the hydroxyl group at position 1 in the sphingosine reduces the capacity for hydrogen bonding in the interfacial region; all this contributes to a more expanded behavior state when compared to ceramides.[17]

The limiting molecular area of ceramides approaches 40 $Å^2$, which is about the minimum cross-sectional area occupied by two closely packed hydrocarbon chains,[50] whereupon chain dispersion interactions are optimized. Even if the tight packing and small hydration confers to relatively long-chain ceramides, some of the highest transition temperature encountered among biologically relevant lipids,[11] shortening of the N-acyl chain length,[35] or presence of unsaturations[51] leads to lower transition temperatures, a more expanded character, and pressure-induced expanded-condensed transitions in monolayers.

Ceramide N-acylated with nervonic acid (C24:1 Δ15) forms condensed films at the air−water interface at 24 °C[50] but with a surface compressional modulus smaller than that of condensed ceramides N-acylated with saturated fatty acids.[14,35] Also, when monolayer temperature is increased up to 30 °C, C24:1 ceramide films display an expanded state and a cooperative expanded-condensed phase transition at 3 mN m^{-1} (data not shown), whereas the shorter N-acyl chain ceramides C14:0 and C16:0 ceramide must be heated up to 37 and 45 °C, respectively, in order to reach similar monolayer states and values of the transition surface pressure.[36] The unsaturation of the N-linked nervonic acid, even when located near the terminal group of the sphingosine base, is thus impairing a tight packing of the hydrocarbon chains. Actually, monolayers of the saturated long chain C24:0 ceramide are very condensed and do not display an expanded phase, even at the highest temperature assayed (50 °C). In the case of the sphingomyelins, films of C24:1 sphingomyelin show an expanded behavior with a diffuse transition to a condensed state at surface pressures above 30 mN m^{-1} (Figure S1 of the Supporting Information), whereas C24:0 sphingomyelin displays a cooperative expanded−condensed transition at 4 mN m^{-1}.

dx.doi.org/10.1021/jp501686q | J. Phys. Chem. B 2014, 118, 7475−7487

The disordering effect of the unsaturated N-bonded nervonic acid to sphingosine-based lipids is also observed in the cerebrosides galactosylceramide[52] and lactosylceramide.[53]

The nature of the N-acyl chain influences not only the monolayer phase behavior and molecular packing of the individual sphingolipids but also their mixing behavior: C16:0 and C24:0 sphingomyelins interacted favorably in binary mixtures with ceramides N-acylated with fatty acyl residues of either the same or increasing hydrocarbon chain length mismatch (C10:0, C16:0, C24:0, and C24:1 ceramides); this is contrary to the binary mixtures of ceramides, in which a strong dependence of the miscibility on the hydrophobic mismatch between the components was observed.[36] The sphingomyelin/ceramide mixtures were characterized by area condensation at low surface pressures and film stiffening at high surface pressures, suggesting not only attractive interactions but also complementary accommodation of the molecules at the interface. Similar packing interactions were observed in binary mixtures, in which one of the components bears a smaller polar headgroup than the other, like the molecular cavity effects described in the mixed films of GM1/Cer[54,55] and GM1/DPPC.[56]

In mixtures of C16:0 sphingomyelin with different ceramides (C10:0, C24:1, and C24:0) at 5 mN m^{-1}, the condensation of the mean molecular area increases linearly with the proportion of ceramide, reaching the maximum effect at a proportion 3:2 (ceramide:sphingomyelin) and remains essentially invariable thereafter, or even decreases in the case of the mixture with C10:0 ceramide. This indicates that at that molar ratio an optimum packing is reached, in which a condensed lattice with enhanced chain interactions is formed. For example, in the case of the mixture C24:1 ceramide/C16:0 sphingomyelin in proportion 3:2 (X_{Cer}= 0.6), the mean area condensation at a surface pressure of 3 mN m^{-1} is 15 $Å^2$, from 58 (ideal value) to 43 $Å^2$ (measured value, Figure 8A), thus, the amount of area condensation of five molecules of sphingomyelin and ceramide in proportion 3:2 in a mixed film is roughly equivalent to an area occupied by one sphingomyelin molecule (almost 75 $Å^2$). Lateral condensation in lipid mixtures occurs when a lattice of usually more expanded molecules can accommodate condensed molecules, and this is reflected in negative excess free energy of mixing; this usually implies a favorable enthalpic compensation for the entropy loss due to the increased ordering of the molecules and to the unfavorably increased electrostatic repulsion brought about in the crowded array of molecular dipoles. The negative excess free energy of mixing of most of sphingomyelin/ceramide mixtures was about 2.8−3.2 kJ mol^{-1} at film compositions X_{Cer} = 0.5−0.6, at which the increase of the surface compressibility modulus and perpendicular dipole moment of the sphingomyelin/ceramide mixtures also reached the maximum values. The hyperpolarization, stiffening, and optical thickening that simultaneously occur indicate that, at such molar ratio, intermolecular interactions through hydrocarbon chain dispersion forces are enhanced, thus leading to mean molecular area reduction.

The mixture formed by C10:0 ceramide/C16:0 sphingomyelin can provide further insights on the molecular interactions and their effect on the lateral packing in the mixture because, at 5 mN m^{-1}, both the components and the mixture form expanded phases. We found that the partial mean molecular area contribution of sphingomyelin in the mixed film was much smaller than its own mean molecular area (80 $Å^2$) at $X_{C10:0\ Cer}$ > 0.4, reaching a value of 30 $Å^2$ at $X_{C10:0\ Cer}$ = 0.9 (Figure S5 of the Supporting Information), which is even less than the value of cross-sectional area occupied by two closely packed all-trans hydrocarbon chains. On the other hand, the partial mean molecular area contribution of C10:0 ceramide at 5 mN m^{-1} at a $X_{C10:0\ Cer}$ = 0.6−0.7 was also smaller but only by 30% of its own mean molecular area (Figure S5 of the Supporting Information). The unrealistically smaller partial molecular area contribution of sphingomyelin to the mean molecular area of the mixture in ceramide-enriched films is due to the strong condensation brought about by the ceramide molecules, which were accommodated in spaces available in the more expanded sphingomyelin lattice (molecular cavity effect) reflected by the above 30% area loss of the ceramide partial contribution to the mean area of the mixed film.

The enhanced van der Waals interactions as a consequence of a closer packing of the acyl chains revealed by the area condensation would contribute as a driving force for favorable mixing, as can be ascertained by analyzing the mixing behavior of C24:1 ceramide with the different sphingomyelins. The acyl chain disorder introduced by the amide-bonded nervonic acid of the ceramide allows this long chain lipid to form mixed expanded phases with sphingomyelins of either short or long N-acyl chain length. The expanded to condensed transition surface pressure in C12:0 sphingomyelin/C24:1 ceramide or C16:0 sphingomyelin/C24:1 ceramide mixtures did not follow a linear variation with the ceramide content in the film (Figure 8D), as was the case for the ceramide binary mixtures like C12:0/C10:0 or even C14:0/C10:0 ceramides, for example.[36] This indicates that enhancement of the hydrocarbon interactions in the mixture of sphingomyelin/ceramide facilitated the condensed phase formation. The latter is also apparent in the mixture of C10:0 ceramide (transition surface pressure of 24 mN m^{-1}) with C16:0 sphingomyelin (transition surface pressure of 18 mN m^{-1}), in which the transition pressure drops down to 10 mN m^{-1} over the range of composition of 0.4 < X_{Cer} < 0.6 (Figure 3D).

The enhancement of the hydrocarbon chain-mediated interactions also determines the amount of maximum area condensation, film stiffening, and hyperpolarization of the mixtures of sphingomyelins with C24:1 ceramide. The more pronounced effects are observed when the N-acyl chain length of the sphingomyelin is increased from C12:0 to C24:0. The longer the N-acyl chain of the sphingomyelins, the higher the molecular interactions with C24:1 ceramide and the effect on the mixing parameters. For example, the positive deviation compared to the ideal behavior of the surface compressibility modulus and perpendicular dipole moment, for the mixture C24:1 ceramide/C24:0 sphingomyelin is about 400 mN m^{-1} and 110 mD, respectively (Figure 8, panels B and C). The increase in the values of these parameters is similar to that obeserved when comparing C10:0 ceramide and C14:0 ceramide, indicating that in the mixture, the equivalent of almost four methylene groups appear to be gained in terms of molecular interactions forces, surface electrostatics, and optical thickness. In fact, an excess free energy of mixing of the C24:1 ceramide/C16:0 sphingomyelin mixture amounting to −2.8 kJ mol^{-1} should be mainly enthalpically driven by the hydrocarbon chain interactions; the four extra methylene groups apparently gained upon mixing would contribute with almost −28 kJ mol^{-1} if a closely packed hexagonal array of hydrocarbon chains in the condensed state is considered.[57] Such enthalpically favorable contribution is large enough for compensating the entropy decrease caused by the increased

dx.doi.org/10.1021/jp501686q | J. Phys. Chem. B 2014, 118, 7475−7487

ordering and the unfavorable dipolar repulsion, thus leading to a favorable excess free energy of mixing.

The surface topography of sphingomyelin/ceramide films was also affected by the enhanced interactions, not only by an increase of the film optical thickness but also by the consequences of hyperpolarization of the interface: condensed domains of large size are formed over the plateau of the compression isotherms of the mixtures that exhibit a transition region. For example, the mixture C24:1 ceramide/C16:0 sphingomyelin shows the largest domains (Figure 9, middle panel) when compared to domains formed during the compression of the mixtures of C16:0 sphingomyelin with either C10:0 (Figure 2B) or C24:0 ceramide (Figure 2A, left panel) or with C12:0 sphingomyelin/C24:1 ceramide (Figure 9, left panel). This is in agreement with the degree of positive deviation of the perpendicular dipole moment of the different mixtures with respect to the ideal behavior and with the difference between the perpendicular dipole moments of the expanded and condensed states of each mixture. In fact, the theory for domain shape equilibrium[58−60] states that the difference in dipole density between the expanded matrix and the overall dipole of the condensed domains determines if flowerlike shapes of increased line tension would form, whereas at lower dipolar density differences among the segregated condensed and expanded phases should lead to round-shaped domains (with lower line tension). In the case of the C24:1 ceramide/C16:0 sphingomyelin mixture, the perpendicular dipole moment value of the expanded state remains at 400 mD and invariant with composition (see isobar at 5 mN m^{-1} at mixture compositions $X_{C24:1\ Cer} < 0.3$ of Figure S4 of the Supporting Information). In the case of the mixed condensed phase, the perpendicular dipole moment depends on the film composition (see isobar at 35 mN m^{-1} at $X_{C24:1\ Cer} > 0.4$ of Figure 8C). Thus, the measured perpendicular dipole moment (450 mD) at 5 mN m^{-1} of the mixture at $X_{C24:1\ Cer} = 0.4$ is actually an average of the two coexisting phases (Figure S4 of the Supporting Information), being about 100 mD of the expanded/condensed dipole density difference; in this mixture, flowerlike domains are formed (Figure 9, middle panel). On the other hand, for the mixed film C10:0 Cer/C24:0 SM, the perpendicular dipole moment of both the expanded and the condensed phases change with the film composition (Figure 5C) and the difference between them is less than 20 mD. Consistently, round-shaped domains are formed over the phase coexistence plateau.

The mixing behavior of the highly dissimilar lipids C10:0 ceramide and C24:0 sphingomyelin is also in keeping with the interpretation of an enhancement of interactions due to complementary packing in an optimal lattice. The larger and more hydrated polar headgroup as well as the asymmetry of the acyl chains both impair a tight packing of sphingomyelin molecules, yielding an expanded matrix in which ceramide with a smaller polar group can be accommodated. On the other hand, the asymmetric C10:0 ceramide, due to the short N-acyl chain, can also forms films in the expanded phase, depending on the surface pressure; both lipids show expanded-to-condensed phase transition at 4 (C24:0 sphingomyelin) and 24 mN m^{-1} (C10:0 ceramide), even though their N-acyl chain length differs in 14 carbons (for comparison the transition surface pressure of C12:0 ceramide having a difference with C10:0 ceramide of only two methylene groups, is about 3.9 mN m^{-1}). C10:0 ceramide is thus able to form mixed expanded phases over the whole compositional range (both with C12:0 ceramide and with C24:0 sphingomyelin), indicating that the degree of order in the phase state is a stronger determinant for the mixing behavior than the hydrophobic mismatch between the components. In a previous work on mixed monolayers of ceramides, it was demonstrated that a difference of 8 carbons in the N-acyl chain length between the molecules led to complete immiscibility between the components, whereas condensed ceramides with a mismatch of just 4 carbons were able to form mixed expanded phases (for example, C14:0/C10:0 ceramides or C16:0/C12:0 ceramides).[36] However, this is not contrary to the present results because, in the case of mixing lipids of the same kind, the phase state of a lipid correlates with the length of the N-acyl chains, and the dependence of the mixing behavior with the hydrophobic mismatch between components can be directly related to differences in their phase state.

The short chain and expanded C12:0 sphingomyelin mixed with C24:1, C12:0, and C14:0 ceramides, while neither molecular area condensation nor film stiffening could be observed with C16:0 or C24:0 ceramides (for brevity, results of mixtures of C12:0 sphingomyelin with C12:0, C14:0, and C16:0 ceramide were not shown). The condensed domains observed by BAM even at the lowest C24:0 ceramide content assayed, with two collapse points occurring at $0.3 < X_{C24:0\ Cer} < 0.6$, indicate macroscopic immiscibility at high surface pressures. Even though the lateral packing of the expanded phase of C12:0 sphingomyelin is similar to that of the other sphingomyelins, the molecular interactions in a mixed lattice of C24:0 ceramide/C12:0 sphingomyelin (either expanded or condensed) appear to be not strong enough for overcoming the self-association tendency of the long-chain ceramide. Thus, even though the hydrophobic mismatch between the components of the mixtures C24:0 ceramide/C12:0 sphingomyelin and C10:0 ceramide/C24:0 sphingomyelin differ by only two methylene groups, the difference in the phase state between a long chain ceramide (very condensed) and a short chain sphingomyelin (expanded) is much higher than in the case of a short chain ceramide (less condensed) and long chain sphingomyelin (less expanded). This can explain why a highly condensed lattice formed by the long chain ceramide in the former system prevents miscibility with the short chain expanded sphingomyelin, whereas the more expanded short chain ceramide allows mixing over the whole range of composition with a more condensed long chain sphingomyelin.

The mixed expanded phases formed by C24:0 ceramide with sphingomyelins with N-acyl chain lengths longer than C12:0, like C16:0 sphingomyelin and C24:1 sphingomyelin (not shown for the sake of clarity), indicates that there is a threshold in the length of the N-acyl chain of sphingomyelin, between C12:0 and C16:0, that can allow favorable interactions in a mixed expanded phase, which appears necessary for dissolving C24:0 ceramide in the condensed state. However, this result was unexpected because the shorter N-acyl chain C16:0 ceramide, which is also condensed at 24 °C, does not form a mixed expanded phase with sphingomyelin even at the lowest amounts of ceramide in the mixture. One possible explanation is that, in the case of N-acyl chains longer than the sphingosine base, the exceeding portion of the hydrocarbon chain may acquire a high degree of conformational freedom, thus yielding an entropic gain to the system that may overcome the tendency to self-association of pure C24:0 ceramide. Thus, asymmetry in the acyl chain length introduces disordering and expanded-like behavior in lipid monolayers of ceramides, as it was previously observed in PCs with the same amount of methylene groups

dx.doi.org/10.1021/jp501686q | J. Phys. Chem. B 2014, 118, 7475−7487

(mixtures of C18/10PC and Di14PC)[61] and enhanced molecular mixing with sphingomyelins.

On the other hand, C12:0 sphingomyelin could readily form a mixed expanded phase with C24:1 ceramide and with a transition surface pressure that also decreased nonlinearly in proportion to the ceramide content in films (Figure 8D), indicating condensed phase stabilization. However, positive deviation from ideality of the mean molecular area (Figure 8A) at 5 mN m^{-1} were observed, which possibly indicate repulsive interactions between the components in the expanded phase and at $X_{C24:1\ Cer} < 0.6$. Partial molar area analysis indicates that, at $X_{C24:1\ Cer} < 0.3$, the ceramide component contributes to the mean area of the mixture with values significantly higher than its own mean molecular area (Figure S6 of the Supporting Information). The latter supports the idea that, in films enriched in C12:0 sphingomyelin, the nervonic ceramide became largely expanded, impairing interactions with the short N-acyl chain sphingomyelin compared with sphingomyelins with longer N-acyl chains. When the mixed expanded phase increases the content in ceramide, nonideal area condensation and film stiffening occurs but only at high ceramide contents in the films ($X_{Cer} > 0.8$, Figure 8A, B), even though hyperpolarization and condensed phase stabilization are already present at $X_{Cer} > 0.3$ (Figure 8, panels C and D). However, the hyperpolarization of the mixture of C24:1 ceramide with C12:0 sphingomyelin is much lower than that observed with the longer sphingomyelins, in keeping with the hydrophobic mismatch between the sphingosine and the N-acyl chains (with possible bending of the longer chains over the shorter one, thus maximizing van der Waals interactions), which would justify the mean molecular area and resultant dipole moments measured, as previously described in films of asymmetric ceramides[35] and galactosylceramides[62] in the condensed state.

Notably, π–A isotherms of C24:1 ceramide/DMPC mixtures[63] showed a remarkably similar behavior to that of mixed films of C24:1 ceramide/C12:0 sphingomyelin and confirm that the comparative overall phase state of the lipids in the mixture, rather than their relative hydrophobic mismatch, is a more important determinant for their mixing. It is interesting to point out that, even though glycerophospholipids lack hydrogen bonding donor capacity, the condensation of the mixed films was similar in mixtures of SM/Cer and PC/Cer. However, when comparing the mixing behavior of C12:0 ceramide in binary films with DiC16:0 PC or C16:0 sphingomyelin, the 1:1 PC/Cer mixture exhibited an expanded to condensed phase transition at 4 mN m^{-1}, whereas the 1:1 mixture of Cer/SM showed only a condensed π–A isotherm (data not shown). Thus, it is likely that favorable interactions between ceramides and sphingomyelins may also involve hydrogen bonding in the polar headgroup region, besides enhanced interactions of the hydrocarbon chains due to complementary packing. The similar behavior of the C24:1 ceramide when mixed with C12:0 SM or DMPC may be explained by a looser packing of the C12:0 sphingomyelin lattice in the Cer/SM mixture, which should weaken hydrogen bonding.

Similar to the polar headgroup-driven miscibility among glycosphingolipids with different oligosaccharide chains,[55] the two-dimensional mixing of the simpler sphingolipids bearing different hydrocarbon moieties is quite complex. Molecular cavity effects and critical lattice distortions in which many sphingolipids can be involved do not only render lateral reorganization in terms of segregation of condensed domains but also in far reaching consequences for the molecular packing, surface hyperpolarization, and elasticity of the interface; these features can also modulate protein insertion and enzyme activities[33] such as dipole potential- and packing-sensitive lipases PLA2.[64,65]

CONCLUSIONS

The mixing behavior of different species of ceramides and sphingomyelins in terms of their N-acyl chain is quite complex and composition-dependent. It shows that "ceramide-enriched domains" formed in mixtures with sphingomyelin cannot be simply conceived as highly condensed and phase-segregated only on the basis of the properties of the more commonly studied analogs and be then extrapolated to all types of ceramide mixtures. Sphingomyelins showed a more expanded behavior than ceramides N-acylated with the same fatty acyl chains, and both types of lipids interacted favorably in monolayers at the air–water interface, even in the presence of the considerable hydrocarbon chain length mismatch. The complementary packing between these sphingolipids led to mean area condensation and film stiffening accompanied by hyperpolarization and optical thickening of the interface in most of the mixtures, which suggest an increased ordering of the hydrocarbon chains upon lipid mixing. The optimal packing of the components in the mixtures enhanced molecular interactions necessary to counterbalance increased dipolar repulsions, indicating that the ordering in the hydrocarbon region is a major factor influencing the mixing behavior of different molecular species of sphingomyelin and ceramide. Surface miscibility depended more on the phase state of the major components than on the hydrophobic mismatch of the acyl chain lengths of the lipids. Total immiscibility could be observed only in the case of the mixture between a short chain sphingomyelin (C12:0 sphingomyelin, fully expanded monolayer) and a long chain ceramide (C24:0 ceramide, fully condensed monolayer), where the high tendency to self-association of ceramide cannot be overcome by mixing in an expanded lattice. The finding that long chain lipids like C24:0 and C24:1, but not C16:0 ceramides, can form mixed expanded phases with different sphingomyelins as a consequence of the acyl chain disorder introduced by the relative asymmetry of the length of the hydrocarbon chains and the resulting overall phase state is a novel finding in the field of membrane biophysics of sphingolipids that challenges the common idea of ceramides as only a solid domain-forming lipid.

ASSOCIATED CONTENT

Supporting Information

The compression isotherms of monolayers of sphingomyelins N-acylated with the fatty acids lauric (C12:0), palmitic (C16:0), lignoceric (C24:0), and nervonic (C24:1) are provided in Figure S1. The mixing behavior of the mixture C16:0 Cer/C16:0 SM are shown in Figure S2 (compression isotherms and composition dependency of the mixing parameters) and Figure S3 (BAM pictures of the mixture films). The perpendicular dipole moment and BAM imaging of the mixture C24:1 ceramide/C16:0 sphingomyelin are shown in Figure S4. Partial molecular areas analysis of the mixtures C10:0 Cer/C16:0 SM and C24:1 Cer/C12:0 SM are shown in Figure S5 and Figure S6, respectively. This material is available free of charge via the Internet at http://pubs.acs.org.

dx.doi.org/10.1021/jp501686q | J. Phys. Chem. B 2014, 118, 7475–7487

AUTHOR INFORMATION

Corresponding Author

*E-mail: fdupuy@fbqf.unt.edu.ar. Tel: +54-381-4248921.

Present Address

†Instituto Superior de Investigaciones Biológicas (INSIBIO), CONICET-UNT, and Instituto de Química Biológica "Dr. Bernabé Bloj", Facultad de Bioquímica, Química y Farmacia, UNT, Chacabuco 461, T4000ILI San Miguel de Tucumán, Argentina.

Notes

The authors declare no competing financial interest.

ACKNOWLEDGMENTS

The authors thank SECyT-UNC, ANPCyT, and CONICET for funding. F.G.D. and B.M. are Career Investigators of CONICET.

REFERENCES

(1) Koynova, R.; Caffrey, M. Phases and Phase Transitions of the Sphingolipids. *Biochim. Biophys. Acta* **1995**, *1255* (3), 213−236.

(2) Maggio, B.; Carrer, D. C.; Fanani, M. L.; Oliveira, R. G.; Rosetti, C. M. Interfacial Behavior of Glycosphingolipids and Chemically Related Sphingolipids. *Curr. Opin. Colloid Interface Sci.* **2004**, *8* (6), 448−458.

(3) Merrill, A. H., Jr. Sphingolipid and Glycosphingolipid Metabolic Pathways in the Era of Sphingolipidomics. *Chem. Rev.* **2011**, *111* (10), 6387−6422.

(4) Boggs, J. M. Lipid Intermolecular Hydrogen Bonding: Influence on Structural Organization and Membrane Function. *Biochim. Biophys. Acta* **1987**, *906* (3), 353−404.

(5) Venkataraman, K.; Futerman, A. H. Ceramide as a Second Messenger: Sticky Solutions to Sticky Problems. *Trends Cell Biol.* **2000**, *10* (10), 408−412.

(6) Slotte, J. P. Biological Functions of Sphingomyelins. *Prog. Lipid Res.* **2013**, *52* (4), 424−437.

(7) Levin, I. W.; Thompson, T. E.; Barenholz, Y.; Huang, C. Two Types of Hydrocarbon Chain Interdigitation in Sphingomyelin Bilayers. *Biochemistry* **1985**, *24* (22), 6282−6286.

(8) Maulik, P. R.; Shipley, G. G. X-Ray Diffraction and Calorimetric Study of N-Lignoceryl Sphingomyelin Membranes. *Biophys. J.* **1995**, *69* (5), 1909−1916.

(9) Carrer, D. C.; Schreier, S.; Patrito, M.; Maggio, B. Effects of a Short-Chain Ceramide on Bilayer Domain Formation, Thickness, and Chain Mobililty: Dmpc and Asymmetric Ceramide Mixtures. *Biophys. J.* **2006**, *90* (7), 2394−2403.

(10) Goni, F. M.; Alonso, A. Biophysics of Sphingolipids I. Membrane Properties of Sphingosine, Ceramides and Other Simple Sphingolipids. *Biochim. Biophys. Acta* **2006**, *1758* (12), 1902−1921.

(11) Fidelio, G. D.; Maggio, B.; Cumar, F. A. Molecular Parameters and Physical State of Neutral Glycosphingolipids and Gangliosides in Monolayers at Different Temperatures. *Biochim. Biophys. Acta* **1986**, *854* (2), 231−239.

(12) Shah, J.; Atienza, J. M.; Rawlings, A. V.; Shipley, G. G. Physical Properties of Ceramides: Effect of Fatty Acid Hydroxylation. *J. Lipid Res.* **1995**, *36* (9), 1945−1955.

(13) Lopez-Montero, I.; Monroy, F.; Velez, M.; Devaux, P. F. Ceramide: From Lateral Segregation to Mechanical Stress. *Biochim. Biophys. Acta* **2010**, *1798* (7), 1348−1356.

(14) Catapano, E. R.; Arriaga, L. R.; Espinosa, G.; Monroy, F.; Langevin, D.; Lopez-Montero, I. Solid Character of Membrane Ceramides: A Surface Rheology Study of Their Mixtures with Sphingomyelin. *Biophys. J.* **2011**, *101* (11), 2721−2730.

(15) Lopez-Montero, I.; Catapano, E. R.; Espinosa, G.; Arriaga, L. R.; Langevin, D.; Monroy, F. Shear and Compression Rheology of Langmuir Monolayers of Natural Ceramides: Solid Character and Plasticity. *Langmuir* **2013**, *29* (22), 6634−6644.

(16) Fanani, M. L.; Maggio, B. Phase State and Surface Topography of Palmitoyl-Ceramide Monolayers. *Chem. Phys. Lipids* **2010**, *163* (6), 594−600.

(17) Pascher, I. Molecular Arrangements in Sphingolipids. Conformation and Hydrogen Bonding of Ceramide and Their Implication on Membrane Stability and Permeability. *Biochim. Biophys. Acta* **1976**, *455* (2), 433−451.

(18) Holleran, W. M.; Takagi, Y.; Uchida, Y. Epidermal Sphingolipids: Metabolism, Function, and Roles in Skin Disorders. *FEBS Lett.* **2006**, *580* (23), 5456−5466.

(19) Moore, D. J.; Rerek, M. E.; Mendelsohn, R. Lipid Domains and Orthorhombic Phases in Model Stratum Corneum: Evidence from Fourier Transform Infrared Spectroscopy Studies. *Biochem. Biophys. Res. Commun.* **1997**, *231* (3), 797−801.

(20) ten Grotenhuis, E.; Demel, R. A.; Ponec, M.; Boer, D. R.; van Miltenburg, J. C.; Bouwstra, J. A. Phase Behavior of Stratum Corneum Lipids in Mixed Langmuir-Blodgett Monolayers. *Biophys. J.* **1996**, *71* (3), 1389−1399.

(21) Barenholz, Y.; Thompson, T. E. Sphingomyelin: Biophysical Aspects. *Chem. Phys. Lipids* **1999**, *102* (1−2), 29−34.

(22) Maulik, P. R.; Shipley, G. G. N-Palmitoyl Sphingomyelin Bilayers: Structure and Interactions with Cholesterol and Dipalmitoylphosphatidylcholine. *Biochemistry* **1996**, *35* (24), 8025−8034.

(23) Sripada, P. K.; Maulik, P. R.; Hamilton, J. A.; Shipley, G. G. Partial Synthesis and Properties of a Series of N-Acyl Sphingomyelins. *J. Lipid Res.* **1987**, *28* (6), 710−718.

(24) Hannun, Y. A.; Obeid, L. M. Many Ceramides. *J. Biol. Chem.* **2011**, *286* (32), 27855−27862.

(25) Zheng, W.; Kollmeyer, J.; Symolon, H.; Momin, A.; Munter, E.; Wang, E.; Kelly, S.; Allegood, J. C.; Liu, Y.; Peng, Q.; Ramaraju, H.; Sullards, M. C.; Cabot, M.; Merrill, A. H., Jr. Ceramides and Other Bioactive Sphingolipid Backbones in Health and Disease: Lipidomic Analysis, Metabolism and Roles in Membrane Structure, Dynamics, Signaling and Autophagy. *Biochim. Biophys. Acta* **2006**, *1758* (12), 1864−1884.

(26) Tettamanti, G.; Bassi, R.; Viani, P.; Riboni, L. Salvage Pathways in Glycosphingolipid Metabolism. *Biochimie* **2003**, *85* (3−4), 423−437.

(27) Hampton, R. Y.; Morand, O. H. Sphingomyelin Synthase and Pkc Activation. *Science* **1989**, *246* (4933), 1050.

(28) Hannun, Y. A.; Bell, R. M. Functions of Sphingolipids and Sphingolipid Breakdown Products in Cellular Regulation. *Science* **1989**, *243* (4890), 500−507.

(29) Hannun, Y. A.; Luberto, C.; Argraves, K. M. Enzymes of Sphingolipid Metabolism: From Modular to Integrative Signaling. *Biochemistry* **2001**, *40* (16), 4893−4903.

(30) Abe, A.; Shayman, J. A.; Radin, N. S. A Novel Enzyme that Catalyzes the Esterification of N-Acetylsphingosine. Metabolism of C2-Ceramides. *J. Biol. Chem.* **1996**, *271* (24), 14383−14389.

(31) De Tullio, L.; Maggio, B.; Fanani, M. L. Sphingomyelinase Acts by an Area-Activated Mechanism on the Liquid-Expanded Phase of Sphingomyelin Monolayers. *J. Lipid Res.* **2008**, *49* (11), 2347−2355.

(32) Jungner, M.; Ohvo, H.; Slotte, J. P. Interfacial Regulation of Bacterial Sphingomyelinase Activity. *Biochim. Biophys. Acta* **1997**, *1344* (3), 230−240.

(33) Maggio, B.; Borioli, G. A.; Del Boca, M.; De Tullio, L.; Fanani, M. L.; Oliveira, R. G.; Rosetti, C. M.; Wilke, N. Composition-Driven Surface Domain Structuring Mediated by Sphingolipids and Membrane-Active Proteins. Above the Nano- but under the Micro-Scale: Mesoscopic Biochemical/Structural Cross-Talk in Biomembranes. *Cell Biochem. Biophys.* **2008**, *50* (2), 79−109.

(34) Shah, J.; Atienza, J. M.; Duclos, R. I., Jr.; Rawlings, A. V.; Dong, Z.; Shipley, G. G. Structural and Thermotropic Properties of Synthetic C16:0 (Palmitoyl) Ceramide: Effect of Hydration. *J. Lipid Res.* **1995**, *36* (9), 1936−1944.

(35) Dupuy, F.; Fanani, M. L.; Maggio, B. Ceramide N-Acyl Chain Length: A Determinant of Bidimensional Transitions, Condensed Domain Morphology, and Interfacial Thickness. *Langmuir* **2011**, *27* (7), 3783−3791.

(36) Dupuy, F.; Maggio, B. The Hydrophobic Mismatch Determines the Miscibility of Ceramides in Lipid Monolayers. *Chem. Phys. Lipids* **2012**, *165* (6), 615−629.
(37) Busto, J. V.; Fanani, M. L.; De Tullio, L.; Sot, J.; Maggio, B.; Goni, F. M.; Alonso, A. Coexistence of Immiscible Mixtures of Palmitoylsphingomyelin and Palmitoylceramide in Monolayers and Bilayers. *Biophys. J.* **2009**, *97* (10), 2717−2726.
(38) Westerlund, B.; Grandell, P. M.; Isaksson, Y. J.; Slotte, J. P. Ceramide Acyl Chain Length Markedly Influences Miscibility with Palmitoyl Sphingomyelin in Bilayer Membranes. *Eur. Biophys J.* **2009**, *39* (8), 1117−1128.
(39) Castro, B. M.; de Almeida, R. F.; Silva, L. C.; Fedorov, A.; Prieto, M. Formation of Ceramide/Sphingomyelin Gel Domains in the Presence of an Unsaturated Phospholipid: A Quantitative Multiprobe Approach. *Biophys. J.* **2007**, *93* (5), 1639−1650.
(40) Pinto, S. N.; Silva, L. C.; Futerman, A. H.; Prieto, M. Effect of Ceramide Structure on Membrane Biophysical Properties: The Role of Acyl Chain Length and Unsaturation. *Biochim. Biophys. Acta* **2011**, *1808* (11), 2753−2760.
(41) Silva, L. C.; de Almeida, R. F.; Castro, B. M.; Fedorov, A.; Prieto, M. Ceramide-Domain Formation and Collapse in Lipid Rafts: Membrane Reorganization by an Apoptotic Lipid. *Biophys. J.* **2007**, *92* (2), 502−516.
(42) Busto, J. V.; Sot, J.; Requejo-Isidro, J.; Goni, F. M.; Alonso, A. Cholesterol Displaces Palmitoylceramide from Its Tight Packing with Palmitoylsphingomyelin in the Absence of a Liquid-Disordered Phase. *Biophys. J.* **2010**, *99* (4), 1119−1128.
(43) Staneva, G.; Chachaty, C.; Wolf, C.; Koumanov, K.; Quinn, P. J. The Role of Sphingomyelin in Regulating Phase Coexistence in Complex Lipid Model Membranes: Competition between Ceramide and Cholesterol. *Biochim. Biophys. Acta* **2008**, *1778* (12), 2727−2739.
(44) Leung, S. S.; Busto, J. V.; Keyvanloo, A.; Goni, F. M.; Thewalt, J. Insights into Sphingolipid Miscibility: Separate Observation of Sphingomyelin and Ceramide N-Acyl Chain Melting. *Biophys. J.* **2012**, *103* (12), 2465−2474.
(45) Brockman, H. L.; Jones, C. M.; Schwebke, C. J.; Smaby, J. M.; Jarvis, D. E. Application of a Microcomputer-Controlled Film Balance System to Collection and Analysis of Data from Mixed Monolayers. *J. Colloid Interface Sci.* **1980**, *78* (2), 502−512.
(46) Gaines, G. *Insoluble Monolayers at Liquid-Gas Interfaces*; Interscience Publishers: New York, 1966.
(47) Ali, S.; Smaby, J. M.; Brockman, H. L.; Brown, R. E. Cholesterol's Interfacial Interactions with Galactosylceramides. *Biochemistry* **1994**, *33* (10), 2900−2906.
(48) Brockman, H. Dipole Potential of Lipid Membranes. *Chem. Phys. Lipids* **1994**, *73* (1−2), 57−79.
(49) Li, X. M.; Smaby, J. M.; Momsen, M. M.; Brockman, H. L.; Brown, R. E. Sphingomyelin Interfacial Behavior: The Impact of Changing Acyl Chain Composition. *Biophys. J.* **2000**, *78* (4), 1921−1931.
(50) Lofgren, H.; Pascher, I. Molecular Arrangements of Sphingolipids. The Monolayer Behaviour of Ceramides. *Chem. Phys. Lipids* **1977**, *20* (4), 273−284.
(51) Peñalva, D. A.; Oresti, G. M.; Dupuy, F.; Antollini, S. S.; Maggio, B.; Aveldaño, M. I.; Fanani, M. L. Atypical Surface Behavior of Ceramides with Nonhydroxy and 2-Hydroxy Very Long-Chain (C28-C32) Pufas. *Biochim. Biophys. Acta, Biomembr.* **2014**, *1838* (3), 731−738.
(52) Smaby, J. M.; Kulkarni, V. S.; Momsen, M.; Brown, R. E. The Interfacial Elastic Packing Interactions of Galactosylceramides, Sphingomyelins, and Phosphatidylcholines. *Biophys. J.* **1996**, *70* (2), 868−877.
(53) Li, X. M.; Momsen, M. M.; Brockman, H. L.; Brown, R. E. Lactosylceramide: Effect of Acyl Chain Structure on Phase Behavior and Molecular Packing. *Biophys. J.* **2002**, *83* (3), 1535−1546.
(54) Carrer, D. C.; Maggio, B. Transduction to Self-Assembly of Molecular Geometry and Local Interactions in Mixtures of Ceramides and Ganglioside Gm1. *Biochim. Biophys. Acta* **2001**, *1514* (1), 87−99.
(55) Maggio, B. Favorable and Unfavorable Lateral Interactions of Ceramide, Neutral Glycosphingolipids and Gangliosides in Mixed Monolayers. *Chem. Phys. Lipids* **2004**, *132* (2), 209−224.
(56) Frey, S. L.; Chi, E. Y.; Arratia, C.; Majewski, J.; Kjaer, K.; Lee, K. Y. Condensing and Fluidizing Effects of Ganglioside Gm1 on Phospholipid Films. *Biophys. J.* **2008**, *94* (8), 3047−3064.
(57) Israelachvili, J. *Intermolecular and Surface Forces*, 3rd ed.; Academic Press: Waltham, MA, 2011.
(58) Gutierrez-Campos, A.; Diaz-Leines, G.; Castillo, R. Domain Growth, Pattern Formation, and Morphology Transitions in Langmuir Monolayers. A New Growth Instability. *J. Phys. Chem. B* **2010**, *114* (15), 5034−5046.
(59) McConnell, H. M. Harmonic Shape Transitions in Lipid Monolayer Domains. *J. Phys. Chem.* **1990**, *94* (11), 4728−4731.
(60) Vega Mercado, F.; Maggio, B.; Wilke, N. Modulation of the Domain Topography of Biphasic Monolayers of Stearic Acid and Dimyristoyl Phosphatidylcholine. *Chem. Phys. Lipids* **2012**, *165* (2), 232−237.
(61) Ali, S.; Smaby, J. M.; Momsen, M. M.; Brockman, H. L.; Brown, R. E. Acyl Chain-Length Asymmetry Alters the Interfacial Elastic Interactions of Phosphatidylcholines. *Biophys. J.* **1998**, *74* (1), 338−348.
(62) Ali, S.; Smaby, J. M.; Brown, R. E. Acyl Structure Regulates Galactosylceramide's Interfacial Interactions. *Biochemistry* **1993**, *32* (43), 11696−11703.
(63) Holopainen, J. M.; Brockman, H. L.; Brown, R. E.; Kinnunen, P. K. Interfacial Interactions of Ceramide with Dimyristoylphosphatidylcholine: Impact of the N-Acyl Chain. *Biophys. J.* **2001**, *80* (2), 765−775.
(64) Maggio, B. Modulation of Phospholipase A2 by Electrostatic Fields and Dipole Potential of Glycosphingolipids in Monolayers. *J. Lipid Res.* **1999**, *40* (5), 930−939.
(65) Perillo, M. A.; Guidotti, A.; Costa, E.; Yu, R. K.; Maggio, B. Modulation of Phospholipases A2 and C Activities against Dilauroylphosphorylcholine in Mixed Monolayers with Semisynthetic Derivatives of Ganglioside and Sphingosine. *Mol. Membr. Biol.* **1994**, *11* (2), 119−126.